Experiment and simulation of creep performance of basalt fibre asphalt mortar under uniaxial compressive loadings

Zhang Xiaoyuan Gu Xingyu Lü Junxiu Zhu Zongkai

(School of Transportation, Southeast University, Nanjing 210096, China)

Abstract: The creep performance of basalt fibre (BF) reinforced in asphalt mortar under uniaxial compressive loadings is investigated. The samples of basalt fibre asphalt mortar (BFAM) with different BF mass fractions (0.1%, 0.2%, and 0.5%) and without BF in asphalt mixture are prepared, and then submitted for the compressive strength test and corresponding creep test at a high in-service temperature. Besides, numerical simulations in finite element ABAQUS software were conducted to model the compressive creep test of mortar materials, where the internal structure of the fibre mortar was assumed to be a two-component composite material model such as fibre and mortar matrix. Finally, the influence factors of rheological behaviors of BFAM are further analyzed. Results indicate that compared to the control sample, the compressive strength of BFAM samples has a significant increase, and the creep and residual deformation are decreased. However, it also shows that the excessive fibre, i. e. with the BF content of 0.5%, is unfavorable to the high-temperature stability of the mortar. Based on the analysis results, the prediction equations of parameters of the Burgers constitutive model for BFAM are proposed by considering the fibre factors.

Key words: basalt fibre; asphalt mortar; uniaxial compressive; creep performance

DOI: 10.3969/j. issn. 1003 - 7985. 2016. 04. 013

Fibre asphalt mortar material, which consists of asphalt mortar and fibre, shows complex thermo-rheological behavior at high temperatures[1]. Adding fibre to the asphalt mortar can fully use the advantages of the asphalt mortar and the fibre, such as stability, reinforcement, crack resistance, and the toughening effects of the fibre, and can greatly improve the performance of the asphalt mixture.

The enhancement effects of fibres on the performance of the asphalt mixture have been studied in previous works. Serfass and Samanos[2] showed that fibres lead to rich asphalt contents, thus the mixture can display high resistance to moisture, aging, and fatigue cracking. Kim et al. [3] evaluated the performance of the polyester fibre-reinforced asphalt mixture by the indirect tensile strength test, and the results indicated that fibres have a significant tensile reinforcing effect. Ye[4] investigated the rheological performance of the asphalt binder and mixture reinforced by lignin fibre, polyester fibre and mineral fibre by the creep test, and the results indicated that fibres can change the viscoelastic properties of materials; i. e., total deformation was decreased during the loading period, and the elastic and retardant elastic deformations were increased. Kumar and Garg[5] showed that the addition of the waste fibre can improve the properties of asphalt binder such as penetration, softening point and ductility.

Basalt fibre (BF) is a high-performance fibre made of basalt rocks which are melted at about 1 500 ℃ and manufactured into continuous fibres. BF has captured the interest of the research community due to its good performance in terms of strength, suitability to a large range of temperatures, and durability. In recent years, BF has been used in asphalt mixture as a strengthening additive[6-8]. Compared with other prevalent additives, such as polyester fibre, glass fibre and lignin fibre, BF has a higher tensile strength, an elastic modulus, and a lower elongation rate. BF retains 95% of its strength under 600 ℃ and is resistant to water, acid, and alkali damage[9]. The high temperature resistance and good chemical stability makes BF an excellent modifier of asphalt mixture.

The performance of asphalt mixture is largely dependent on its components as a composite material. In particularly, binding materials play an important role, which includs asphalt binder, asphalt mastic, and asphalt mortar. The research on the stabilizing and reinforcing effects of fibres on the performance of the components in asphalt mixture has been a focus[10-14].

However, most studies focused on the performance of fibre-reinforced asphalt mixture or asphalt mastic, and limited work described the effects of BF on the asphalt mortar. In this paper, BF is added into the asphalt mortar as an additive to prepare fibre-reinforced binding materials. The specimens of basalt fibre asphalt mortar (BFAM) are prepared with various BF contents, and then

Received 2016-05-19.

Biographies: Zhang Xiaoyuan (1986—), male, graduate; Gu Xingyu (corresponding author), male, doctor, associate professor, guxingyu1976@163.com.

Foundation item: The National Natural Science Foundation of China (No. 51108082).

Citation: Zhang Xiaoyuan, Gu Xingyu, Lü Junxiu, et al. Experiment and simulation of creep performance of basalt fibre asphalt mortar under uniaxial compressive loadings[J]. Journal of Southeast University (English Edition), 2016, 32(4): 472 - 478. DOI: 10.3969/j. issn. 1003 - 7985. 2016. 04. 013.

tested at high temperatures using the uniaxial compressive strength test and corresponding creep test. The effect of BF is analyzed by comparing the testing results of BFAM with plain material. Numerical simulation in finite element (FE) ABAQUS software is also performed to model the compressive creep tests of mortar materials, where the internal structure of the fibre-reinforced materials is considered to build a two-phase composite material composed of fibre and mortar matrix. The creep performance of the model are further investigated under uniaxial compressive loadings to evaluate the influence factors of BF to the deformation resistance of the mortar materials at a high in-service temperature.

1 Materials

1.1 Raw materials

SBS modified asphalt of PG76-22 grade is used in asphalt mortar. Mineral powder and fine aggregate are limestone and basalt, respectively. According to the standard JTG E42—2005[15] and JTG E20—2011[16], the properties of component materials are obtained, and the properties of the BF are shown in Tab. 1.

Tab. 1 Properties of basalt fibre

Fibre	Tensile strength/ MPa	Elastic modulus/ GPa	Elongation rate/%
Basalt fibre	4500	100	3.1
Polyester fibre	750	13	12
Lignin fibre	580	5.5	18

1.2 Asphalt mortar gradation

In order to study the effect of BF on asphalt mortar, asphalt mortar and the corresponding asphalt mixture should be prepared. Since the asphalt mixture with fibre is used in the upper and middle course of the asphalt pavement, the asphalt mortar of AC-13 gradation usually used in the upper course of the pavement is selected in this paper. Referring to the corresponding specification JTG F40—2004 for the AC-13 aggregate gradation, the aggregate size of asphalt mortar is less than 4.75 mm. The asphalt mixture and corresponding mortar gradation are shown in Tab. 2.

Tab. 2 Asphalt mixture and mortar for AC-13 gradation

Sieve size/mm	2.36	1.18	0.6	0.3	0.15	0.075	<0.075
Retained percentage of AC-13 gradation	16	10.5	7.5	5.5	3.5	4	6
Retained percentage of asphalt mortar gradation	30.2	19.8	14.2	10.4	6.6	7.5	11.3

1.3 Basalt fibre content

Fibre content is usually calculated by the mass fraction of asphalt mixture, so the percentage of fibre content in asphalt mortar can be obtained by the relationship between asphalt mortar and its asphalt mixture in terms of fiber content. In the present paper, the BF content are 0.1%, 0.2% and 0.5% in asphalt mixture, and correspondingly, 0.19%, 0.38% and 0.95% in asphalt mortar.

2 Tests and Results

For high-temperature performance tests, specimens were fabricated by the Superpave gyratory compactor. After adding fibres into the asphalt mortar, fibres may absorb a certain asphalt to make the bonding between aggregate and asphalt insufficient, which leads to an increase in the difficulty of specimen moulding, so the bitumen-aggregate ratio of asphalt mortar is adjusted to 8.9%, 9.0%, 9.1%, and 9.4%; correspondingly, the BF contents are 0%, 0.1%, 0.2%, and 0.5%, respectively. The diameter and height of the cylindrical specimens are all 100 mm. The uniaxial compression test is performed by a loading instrument UTM-25 with a loading rate of 2 mm/min at 60 ℃, where two replicates are tested to obtain the average values of specimens for each fiber content.

2.1 Compression strength test

The compression strength equation of BFAM is given as

$$R_c = \frac{4P}{\pi d^2} \tag{1}$$

where R_c denotes the compressive strength, MPa; P is the maximum loads, N; d is the diameter of the specimen, mm.

Fig. 1 indicates that the compressive strength increases with the increase in BF content within 0.2% BF content, where the peak stress is improved by 31.7% more than that of the control specimen, but the corresponding strain is not decreased, so BF is advantageous for the high-temperature stability of asphalt mortar. However, when the fibre content is 0.5%, the compressive strength of the BFAM sample will be decreased, which is even lower than

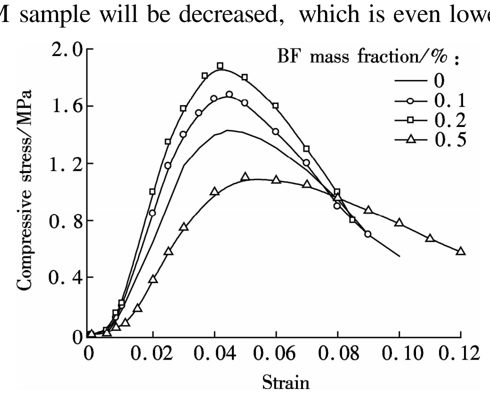

Fig. 1 Curve of uniaxial compressive stress and its strain at different BF mass fractions

the result of the control specimen. It also shows that excessive fibre is unfavorable to the high-temperature stability of the mortar, and the compressive strength with 0.5% BF content specimens is decreased by approximately 23% compared to the control sample. Based on the experimental results, it is proven that appropriate amounts of fibre additive can effectively enhance the strength of asphalt mortar, but excessive fibres will decrease the bonding between asphalt and other components.

2.2 Compression creep test

Uniaxial compressive creep can be seen as a process of deformation increasing with time under a constant uniaxial load. In this paper, the loading stress of BFAM specimens is set to be 20% and 30% of the compression strength of the control specimen, namely, 0.28 and 0.42 MPa, respectively. The creep loading was performed by keeping to 30 min, and then the creep unloading was conducted for about 10 min, where the maximum compressive creep deformation is seen to be the peak value during the loading process. The elastic and delay viscoelastic deformation are removed by unloading to obtain the residual creep deformation.

Fig. 2 shows that the peak strain and the residual strain of BFAM samples first decrease and then increase with the increase in fibre content. Compared with the control specimen, the BFAM specimen can make the creep deformation of asphalt mortar smaller and improve the deformation recovery rate, so it has a good high-temperature stability. However, when the BF content increases to 0.5%, the creep peak deformation, the creep rate, and the residual deformation all increase, and the high-temperature performance is decreased. This finding also indicates that the BF in an appropriate content range can improve the performance of asphalt mortar.

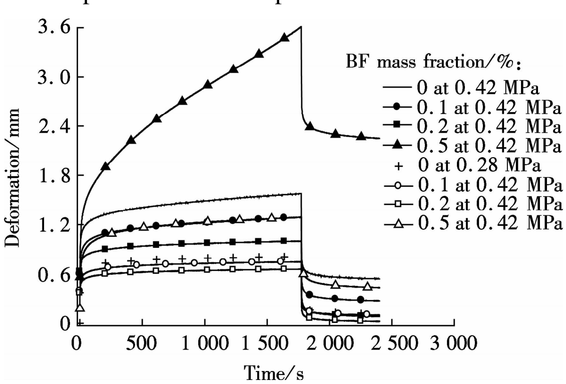

Fig. 2 Relationship of deformation with time

3 Numerical Simulation

3.1 Burgers model

The Burgers constitutive model of asphalt materials can be obtained using a combination of the basic viscoelastic models. The constitutive and creep equations of the model are as follows:

$$\sigma + p_1\dot{\sigma} + p_2\dot{\sigma} = q_1\dot{\varepsilon} + q_2\ddot{\varepsilon} \tag{2}$$

$$\varepsilon(t) = \sigma_0\left[\frac{1}{E_1} + \frac{t}{\eta_1} + \frac{1}{E_2}(1 - e^{-E_2/\eta_2 t})\right] \tag{3}$$

where $p_1 = (\eta_1 E_1 + \eta_1 E_2 + \eta_2 E_1)/(E_1 E_2)$; $p_2 = \eta_1\eta_2/(E_1 E_2)$; $q_1 = \eta_1$; $q_2 = \eta_1\eta_2/E_2$; E_1, η_1 are the elastic modulus and viscosity indices in the Maxwell model, respectively; E_2, η_2 are the elastic modulus and viscosity indices in the Kelvin model, respectively. In this paper, the viscoelastic parameters of asphalt mortar can be obtained by the compressive creep test.

3.2 Implementation of the model in ABAQUS

In the FE ABAQUS software, the mechanical behavior of viscoelastic materials can be characterized by relaxation modulus parameters with the Prony series form, including the time domain and the frequency dependence types. This research adopts the former with the shear relaxation modulus to describe the viscoelasticity of asphalt mortar. The viscoelastic parameters with the Prony series form can be represented as follows:

$$G(t) = G_\infty + \sum_{i=1}^{n} G_i e^{-t/\tau_i} \tag{4}$$

where G_∞, G_i are the shear moduli; τ_i is the shear relaxation time in series components.

The transformation steps of the Burgers model parameters are as follows:

1) The conversion between the shear modulus and the elastic modulus can be obtained as

$$G_1 = \frac{E_1}{2(1+u)} \tag{5}$$

$$G_2 = \frac{E_2}{2(1+u)} \tag{6}$$

2) The relaxation modulus can be obtained by the Laplace transform of the constitutive relationship,

$$\bar{Y}(s) = \frac{q_1 s + q_2 s^2}{s(1 + p_1 s + p_2 s^2)} \tag{7}$$

In addition, the relaxation modulus is obtained by the inverse Laplace transformation in a time domain,

$$Y(t) = \frac{q_2}{p_2(\alpha - \beta)}\left[\left(\alpha - \frac{q_1}{q_2}\right)e^{-\alpha t} + \left(\frac{q_1}{q_2} - \beta\right)e^{-\beta t}\right] \tag{8}$$

Moreover, the shear modulus is

$$G(t) = 0.5Y(t) = \frac{G_1}{\alpha - \beta}\left[\left(\frac{G_2}{\eta_2} - \beta\right)e^{-\beta t} - \left(\frac{G_2}{\eta_2} - \beta\right)e^{-\alpha t}\right] \tag{9}$$

The normalized processing is

$$G(t) = G_\infty + G_0(g_1 e^{-t/\tau_1} + g_2 e^{-t/\tau_1}) \tag{10}$$

where $G_\infty = 0$; $G_0 = G_1$; $g_1 = \frac{1}{\alpha-\beta}\left(\frac{G_2}{\eta_2}-\beta\right)$; $g_2 = \frac{-1}{\alpha-\beta}\left(\frac{G_2}{\eta_2}-\alpha\right)$; $\tau_1 = \frac{1}{\beta}$; $\tau_2 = \frac{1}{\alpha}$; $\alpha = \frac{1}{2p_2}(p_1 + \sqrt{p_1^2-4p_2})$; $\beta = \frac{1}{2p_2}(p_1 - \sqrt{p_1^2-4p_2})$. Through the above conversion method, the four parameters of the Burgers model obtained by fitting the curve of strain with time are converted into the shear relaxation modulus in the Prony series form, so that the viscous-elastic material parameters g_1, g_2, τ_1, τ_2 can be implemented in ABAQUS, where g_i is the shear coefficients of relaxation modulus; u is the Poisson's ratio.

3.3 Simulation of asphalt mortar

The uniaxial compressive creep test for the control sample is simulated by ABAQUS software, and the diameter and height of the cylindrical samples are all set to be 100 mm. The viscoelastic parameters of the Burgers model and the compressive loading of the sample top in the creep test simulation are listed in Tab. 3.

Tab. 3 Parameter values for asphalt mortar at 60℃

Parameters	E_1/MPa	E_2/MPa	η_1/(MPa · s)	η_2/(MPa · s)	g_1	g_2	τ_1	τ_2	Compressive stress/MPa
Values	49.5	155.3	697 062	12 950	0.24	0.76	63.2	18 324	0.28

The 3D stress contour and the vertical deformation of the specimens after 1 800 s are shown in Figs. 3 and 4, respectively. For the vertical deformation, the comparison results of testing and simulation are shown in Fig. 5, indicating that the simulation results have a good agreement with the experimental results. Consequently, the mechanical model and the selected parameters are reasonable, and the simulation of BF added into the mortar matrix using the Burgers model in ABAQUS can be used for further numerical simulations.

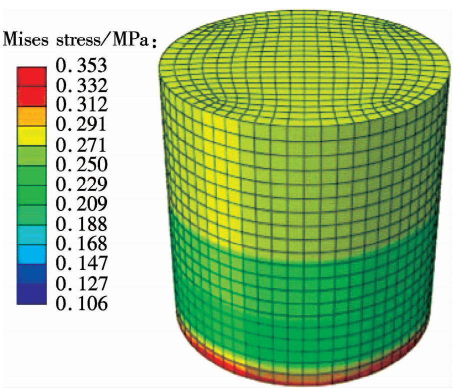

Fig. 3 3D stress contour under a creep loading

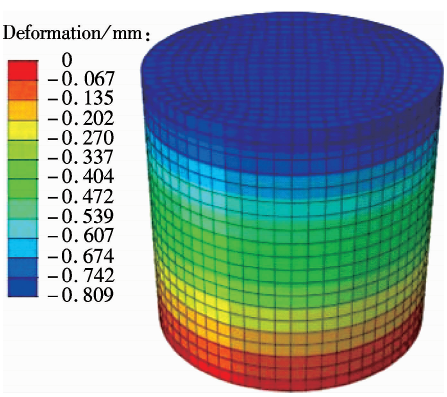

Fig. 4 Vertical creep deformation contour

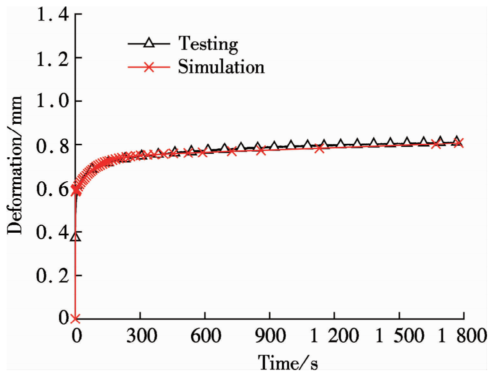

Fig. 5 Results of testing and simulation for asphalt mortar

3.4 Simulation of BFAM

BFAM can be considered as a composite material composed of two components including the BF and asphalt mortar matrix. On the basis of asphalt mortar simulation, fibres are embedded into mortar matrix to form BFAM composites, which is used for further numerical simulating and investigating the creep performance of BFAM at a high in-service temperature.

When simulating the uniaxial compressive creep test for BFAM, fibres should be as possibly as uniformly distributed in the mortar matrix. In addition, the deformation of the top surface of the BFAM samples should be uniform. Based on the previous numerical model, a rigid pressure head is added to the top surface of samples with smooth interaction to achieve uniform deformation. Moreover, before conducting numerical simulations of BFAM, the total number of fibres should be obtained. Nevertheless, the total fibre volume compared with the mortar volume is very small, so this research does not adopt the basic calculation formula to obtain the total fibre volume. It can be calculated by the ratio of the total content of fibres and the content of a single fibre. For example, when fibre contents are 0.1% and 0.2%, the total numbers of fibres are approximately 494×10^3 and 988×10^3.

For convenience, BFs bound as fibre bundles are embedded in the mortar matrix. When the BF content is 0.1%, the amount of the fibre bundles is about 308, 403, and 548 and the sizes of the fibre bundles are 0.8 mm × 0.8 mm, 0.7 mm × 0.7 mm, 0.6 mm × 0.6 mm in width and height and 6 mm in the same length, respectively. The fibre bundles of 0.8 mm × 0.8 mm × 6 mm (type Ⅰ) and 0.6 mm × 0.6 mm × 6 mm (type Ⅱ) with 0.1% BF content are investigated.

For type Ⅰ, the fibre arrangement along the longitudinal direction is divided into three layers with about 100 fibre bundles in each layer, as shown in Fig. 6(a). The calculated displacement contour is shown in Fig. 6(b), indicating that the top deformation of simulation is close to that of the test. For type Ⅱ, the fibre arrangement along the longitudinal direction is divided into seven layers at a 12 mm spacing between layers with about 75 fibre bundles in each layer, as shown in Fig. 7(a). Fig. 7(b) indicates that the top deformation of type Ⅱ BFAM is smaller than that of type Ⅰ; i. e., the deformation decreases from 0.747 to 0.695 mm. For the fibre arrangement of 0.2% BF content, referring to the methods of 0.1% BF content, the number of the fibre layers increased by twice or the distance at the interlayer was reduced by half.

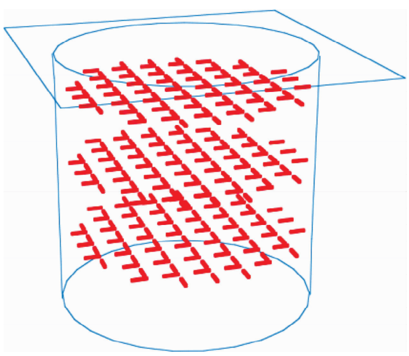

(a)

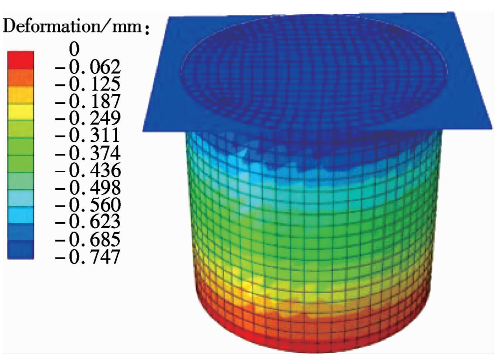

(b)

Fig. 6 Deformation of BFAM sample of type Ⅰ. (a) Fibre arrangement along the longitudinal; (b) Deformation contour

The results of simulation with different BF contents and fibre sizes are listed in Tab. 4. It is found that the compressive creep deformation of type Ⅰ at 1 800 s is closer to the value of testing compared with that of type Ⅱ, so

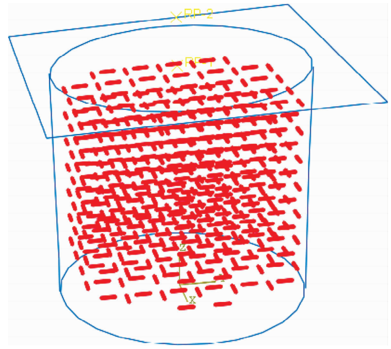

(a)

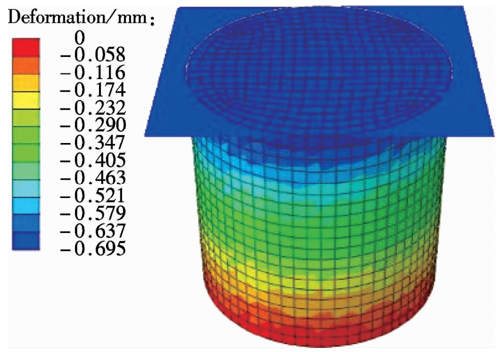

(b)

Fig. 7 Deformation of BFAM samples of type Ⅱ. (a) Fibre arrangement along longitudinal; (b) Deformation contour

Tab. 4 Results of the compressive deformation at 1 800 s and 60 ℃ under 0.28 MPa

Fibre mass fraction/%	Dimension/ mm × mm × mm	Fibre number	Deformation/mm	
			Simulation	Testing
0			0.807	0.811
0.1	0.6 × 0.6 × 6	525	0.695	0.737
	0.8 × 0.8 × 6	300	0.747	
0.2	0.6 × 0.6 × 6	1 050	0.593	0.657
	0.8 × 0.8 × 6	600	0.651	

the dimension of type Ⅰ in the asphalt mortar model is feasible, and the relaxation modulus with the Prony series form characterizing viscoelastic behaviors of BFAM is effective.

3.5 Discussion and analysis

Combining the testing results with the simulation results of the creep behaviors of BFAM, the effect of BF on asphalt mortar at 60 ℃ was analyzed. In this study, four parameters E_1, E_2, η_1, and η_2 of the Burgers model were used to reflect viscoelastic creep behaviors, and the influence factors such as fibre content and modulus were considered under uniaxial compressive loadings. Under a compressive stress of 0.28 MPa, the relationship of the four parameters E_1, E_2, η_1, and η_2 with influencing factors are shown in Figs. 8 and 9.

Finally, the prediction equations of parameters of the Burgers model can be obtained by considering various influencing factors, which are described as follows:

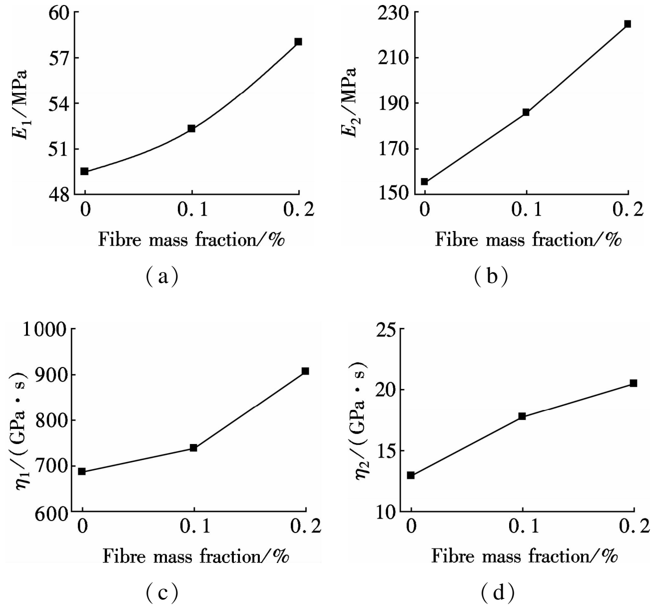

Fig. 8 Relationship of four parameters of the Burgers model and fibre mass fraction under the fibre modulus of 100 MPa. (a) E_1; (b) E_2; (c) η_1; (d) η_2

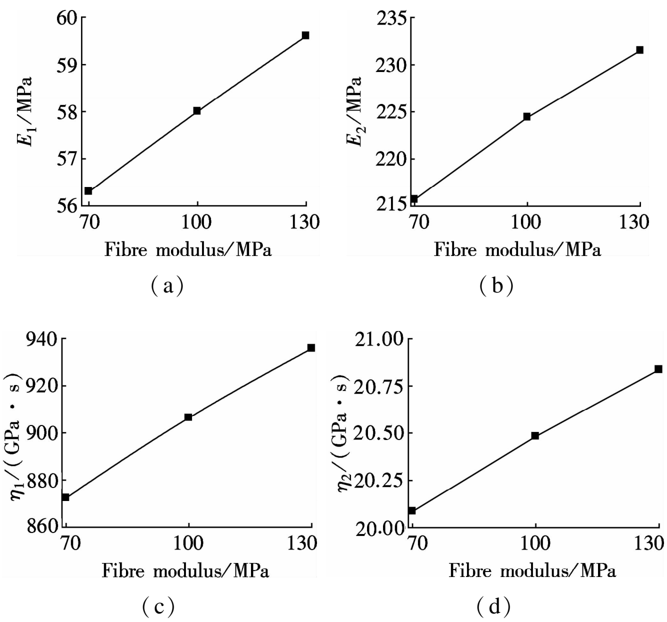

Fig. 9 Relationship of four parameters of the Burgers model and fibre modulus under the fibre mass fraction of 0.2%. (a) E_1; (b) E_2; (c) η_1; (d) η_2

$$E_1(a,\ b) = 42.5a + 0.55a/2 \times (b - 100) + 49.01 \tag{11}$$

$$E_2(a,\ b) = 345.5a + 2.63a/2 \times (b - 100) + 153.9 \tag{12}$$

$$\eta_1(a,\ b) = 1\,096\,553a + 10\,545a/2 \times (b - 100) + 696\,075 \tag{13}$$

$$\eta_2(a,\ b) = 37\,654a + 125.1a/2 \times (b - 100) + 13\,294 \tag{14}$$

where a represents the fibre mass fraction, %; and b denotes the fibre modulus, MPa. The effect of a and b on asphalt mortar are assumed to be independent from each other in the above equations.

From the above equations and Figs. 8 and 9, the changing rule of the parameters of the Burgers model is similar under high in-service temperatures. The parameters of the Burgers model have a positive correlation with the fibre content and its modulus.

4 Conclusion

1) Based on the results of the compressive strength test of asphalt mortar, it is found that the high-temperature compressive strength and the peak stress increase with the increase of fibre contents, but the corresponding strain is not decreased. However, when the BF content is 0.5%, the peak stress of specimens is decreased compared with that of the control specimen.

2) Based on the results of the compressive creep test of asphalt mortar, it can be found that the creep and the residual deformation decrease and the creep stiffness modulus increases with the increase of the BF content. The peak creep and its residual deformation are all decreased, and the peak stiffness modulus is increased. However, when the BF content is 0.5%, the creep and the residual deformations of BFAM are increased compared to those of the control specimen, and the creep stiffness modulus is lower than that of the control specimen. Therefore, it is concluded that an appropriate content of the BF (less than 0.5%) added into asphalt mortar can improve the high-temperature stability of asphalt mortar.

3) Based on the results of numerical simulations, it shows that compared to the control sample, the axial deformation of BFAM is significantly increased, and the simulation results are in good agreement with testing results. Finally, the equations of the relationship between each parameter of the Burgers model and influence factors of fiber are established at 60 ℃.

References

[1] Wang J Y, Qian Z D. Indirect tension test of epoxy asphalt mixture using microstructural finite-element model [J]. *Journal of Southeast University (English Edition)*, 2011, **27**(1): 65 - 69.

[2] Serfass J P, Samanos J. Fiber-modified asphalt concrete: characteristics, applications and behavior [J]. *Journal of the Association of Asphalt Paving Technologists*, 1996, **65**, 193 - 230.

[3] Kim K W, Doh Y S, Lim S. Mode I reflection cracking resistance of strengthened asphalt concretes [J]. *Construction and Building Materials*, 1999, **13**(5), 243 - 251. DOI:10.1016/s0950-0618(99)00032-x.

[4] Ye Q. Research on the rheological characteristics of fiber modified asphalt binder and mixture [D]. Wuhan: School of Materials Science and Engineering, Wuhan

University of Technology, 2007. (in Chinese)
[5] Kumar P, Garg R. Rheology of waste plastic fibre-modified bitumen [J]. *International Journal of Pavement Engineering*, 2011, **12**(5): 449 - 459. DOI: 10.1080/10298430903255296.
[6] Wei Y, Zhang Z, Si W, et al. Performance promoting mechanism of asphalt mixture by basalt fiber [J]. *Journal of Chang'an University*, 2012, **32**(2): 39 - 44. (in Chinese)
[7] Zhao L. Study on the influence mechanism of basalt fiber on asphalt mixture property [D]. Dalian: School of Civil Engineering and Hydraulic Resources, Dalian University of Technology, 2013. (in Chinese)
[8] Morova N. Investigation of usability of basalt fibers in hot mix asphalt concrete [J]. *Construction and Building Materials*, 2013, **47**: 175 - 180. DOI: 10.1016/j.conbuildmat.2013.04.048.
[9] Wang D, Wang L, Gu X, et al. Effect of basalt fiber on the asphalt binder and mastic at low temperature [J]. *Journal of Materials in Civil Engineering*, 2013, **25**(3): 355 - 364. DOI: 10.1061/(asce)mt.1943-5533.0000605.
[10] Bonnetti K, Nam K, Bahia H. Measuring and defining fatigue behavior of asphalt binders [J]. *Transportation Research Record*, 2002, **1810**: 33 - 43. DOI: 10.3141/1810-05.
[11] Kandhal P, Lynn C, Parker F. Characterization tests for mineral fillers related to performance of asphalt paving mixtures [J]. *Transportation Research Record*, 1998, **1638**: 101 - 110. DOI: 10.3141/1638-12.
[12] Kim Y R, Allen D H, Little D N. Computational constitutive model for predicting nonlinear viscoelastic damage and fracture failure of asphalt concrete mixtures [J]. *International Journal of Geomechanics*, 2007, **7**(2): 102 - 110. DOI: 10.1061/(asce)1532-3641(2007)7:2(102).
[13] Xu T, Ni F. Rheological behavior of basalt fiber reinforced asphalt mastic [J]. *Journal of Wuhan University of Technology (Material Science Edition)*, 2014, **29**(5): 950 - 955. DOI: 10.1007/s11595-014-1026-0.
[14] Wu M M, Li R, Zhang Y Z, et al. Stabilizing and reinforcing effects of different fibers on asphalt mortar performance [J]. *Petroleum Science*, 2015, **12**(1): 189 - 196. DOI: 10.1007/s12182-014-0011-8.
[15] Ministry of Transport of the People's Republic of China. Standard JTG E42—2005. Test methods of aggregate for highway engineering [S]. Beijing: China Communications Press, 2005. (in Chinese)
[16] Ministry of Transport of the People's Republic of China. Standard JTG E20 - 2011. Standard test methods of bitumen and bituminous mixtures for highway engineering [S]. Beijing: China Communications Press, 2011. (in Chinese)

单轴受压下玄武岩纤维沥青砂浆流变性能试验及仿真

张小元　顾兴宇　吕俊秀　朱宗凯

(东南大学交通学院, 南京 210096)

摘要:研究了玄武岩纤维加筋沥青砂浆在单轴受压作用下的流变性能. 首先,通过制备加质量分数为 0.1%, 0.2%, 0.5% 的沥青混合料纤维和不加纤维的沥青砂浆试件,实施了高温条件下的压缩强度试验和相应蠕变试验. 结果表明,相较于纯沥青砂浆,纤维砂浆的抗压强度有较大提高,蠕变变形和相应的残余变形降低,但当纤维过量时,即 0.5% 纤维含量,其性能反而不利. 同时,利用有限元 ABAQUS 软件开展了纤维加砂浆两相复合材料的流变模拟,得到模拟与试验相一致的结果,并分析了纤维模量与含量对砂浆流变特性的影响. 基于上述分析结果提出了纤维影响因素的 Burgers 本构模型参数预测方程.

关键词:玄武岩纤维;沥青砂浆;单轴受压;流变性能

中图分类号:U416